

Fig. 3 — Nitrogen saturation concentration as a function of oxygen concentration.

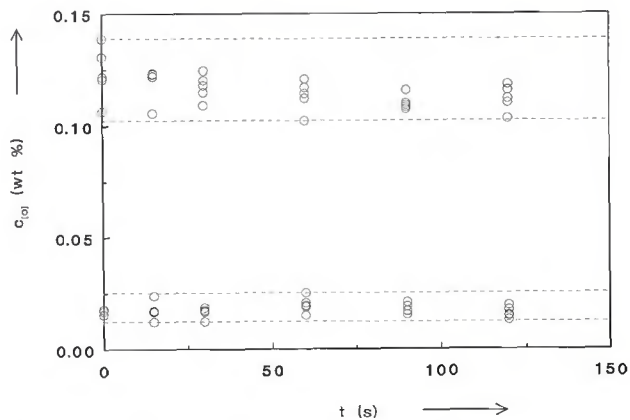


Fig. 4 — Oxygen concentration as a function of degassing time for two series of samples with different initial oxygen concentrations.

tion of degassing time. Again each point represents the average of at least five measurements. Figure 5 clearly shows that the nitrogen concentration decreases with degassing time, the decrease being slower when more oxygen is present in the liquid metal. Obviously, oxygen hampers the desorption of nitrogen.

The results described in the foregoing seem to suggest that the effect of oxygen on the nitrogen absorption is directly related to the surface activity of oxygen. In particular, it appears that the oxygen at the surface impedes the escape of nitrogen, giving rise to higher nitrogen levels in the material.

In order to verify this conclusion and to obtain more quantitative insight in the role of oxygen, the mechanism of nitrogen absorption during arc melting will be considered in more detail.

Recently, Den Ouden and Griebeling (Ref. 11) proposed a simple model of nitrogen absorption during arc welding. According to their model, the nitrogen concentration in the melt is the result of

two mutually independent processes: inflow and outflow. Inflow of nitrogen takes place exclusively through the interface between the arc and the liquid metal, the inflow rate being determined by the arc conditions (notably the partial pressure of the nitrogen in the arc and the temperature of the arc). Outflow of nitrogen takes place through the entire outer surface of the liquid metal (including that part of the surface which is covered by the arc), the outflow rate being proportional to the nitrogen concentration in the liquid metal. On this basis, the time-dependent change in nitrogen concentration can be described by the equation

$$\frac{dN}{dt} = W \frac{dc}{dt} = \alpha A - \beta Bc \quad (1)$$

with  $N$  the amount of nitrogen present in the liquid metal,  $c$  the nitrogen concentration in the liquid metal,  $t$  the time,  $W$  the sample weight,  $A$  the interface area between the arc and the liquid metal,  $B$  the interface area between the

liquid metal and the surrounding gas phase,  $\alpha$  the inflow coefficient (the amount of nitrogen entering the liquid metal per unit area per unit time) and  $\beta$  the outflow coefficient (the amount of nitrogen leaving the liquid metal per unit area per unit time).

The solution of differential Equation 1 can be written as:

$$c(t) = \frac{\alpha A}{\beta B} \left[ 1 - \exp\left(-\frac{\beta B}{W} t\right) \right] \quad (2)$$

Saturation occurs when the amount of nitrogen entering the liquid metal per unit time equals the amount of nitrogen leaving the liquid metal per unit time. The saturation value  $c_s$  can be obtained by substituting  $t = \infty$  in Equation 2, which leads to:

$$c_s = \frac{\alpha A}{\beta B} \quad (3)$$

Using Equations 1, 2 and 3 and the experimental data presented in Figs. 2 and 5, values of  $\alpha$  and  $\beta$  were calculated

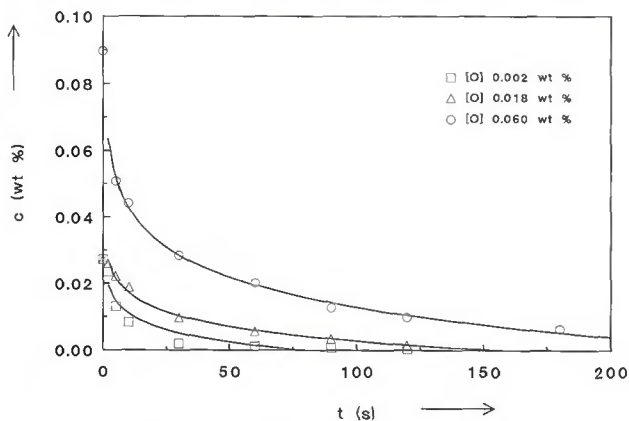


Fig. 5 — Nitrogen concentration as a function of degassing time for three series of samples with different oxygen concentrations.

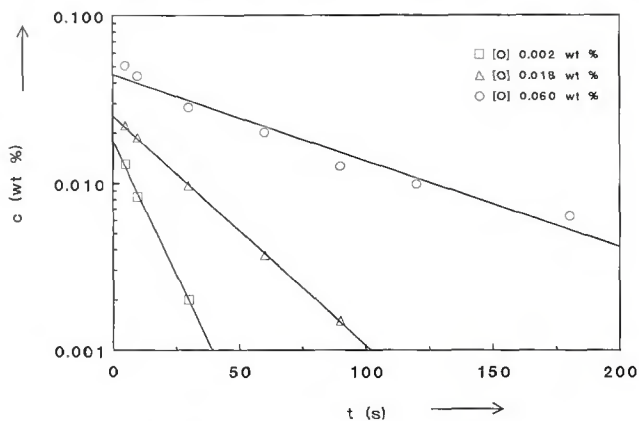


Fig. 6 — Logarithm of nitrogen concentration as a function of degassing time for three samples with different initial nitrogen concentrations (semilogarithmic plot of the experimental data presented in Fig. 5).

**Table 2 — The Inflow Coefficient  $\alpha$  and the Outflow Coefficient  $\beta$  for Samples with Different Oxygen Concentrations**

[O] (wt-%)	$\alpha$ (g/sm <sup>2</sup> )	$\beta$ (g/sm <sup>2</sup> )
0.002	0.55	$0.95 \times 10^3$
0.018	0.52	$0.40 \times 10^3$
0.060	0.45	$0.13 \times 10^3$

as follows:

First, the linear plot of Fig. 5 (nitrogen concentration vs. degassing time) was converted to the semilogarithmic plot of Fig. 6 (logarithm of nitrogen concentration vs. degassing time). In this semilogarithmic plot, nitrogen concentrations below 0.001 wt-% have been omitted. As can be seen, the experimental data presented in Fig. 6 can be easily approximated by straight lines. From the slope of these lines and measured values of  $B$ , values of  $\beta$  were calculated with the help of Equation 2, taking into account that  $\alpha = 0$  (degassing).

From the obtained values of  $\beta$  and the saturation concentrations  $c_s$  given in Fig. 2, values of  $\alpha$  were calculated using Equation 3. In Table 2, values of  $\alpha$  and  $\beta$  calculated in this way are given for the three oxygen levels. It appears that  $\alpha$  decreases only slightly, whereas  $\beta$  decreases rapidly with increasing oxygen level. This leads to the conclusion that oxygen influences the nitrogen absorption predominantly through its effect on the outflow rate, with its effect on the inflow rate being negligibly small.

This behavior can be understood by assuming that, as in the case of nonarc melting of iron and steel (Refs. 14, 15), oxygen forms an electrostatic double-layer of  $O^{2-}$  and  $Fe^{2+}$  on the surface of the liquid metal, which hampers the passage of nitrogen atoms. Directly under the arc, this surface layer is virtually destroyed due to the high temperature of the arc plasma and by the impinging plasma jet so that the inflow rate will scarcely be affected. However, outside the arc the surface layer remains intact and the escape of nitrogen atoms (*i.e.*

the outflow) is hampered.

As can be seen in Fig. 3, oxygen is only active in the concentration range up to approximately 0.08 wt-%. Increasing the oxygen concentration above this level does not affect the nitrogen absorption any further. This can be understood by assuming that the oxygen layer at the surface of the liquid metal builds up with increasing oxygen concentration until at a level of 0.08 wt-% the formation of the layer is completed.

It is interesting to note that in melting experiments under nonarc equilibrium conditions (Refs. 14, 15), the threshold level above which the oxygen is not active any more is considerably smaller (0.02–0.04 wt-%) than that found in the present work under arc melting conditions (0.08 wt-%). This apparent discrepancy can be explained by realizing that in the case of arc melting more vigorous stirring of the liquid metal occurs. This type of stirring is due to electromagnetic- and surface tension-induced forces (Ref. 16) that are absent in the case of nonarc melting. Due to stirring of the liquid metal in the case of arc melting, a higher overall oxygen concentration is required for the surface to be completely covered by an oxygen layer.

## Conclusions

On the basis of the results presented in this paper, the following conclusions can be drawn:

1) The absorption of nitrogen during arc melting and arc welding of iron is strongly affected by the presence of oxygen in the material: the nitrogen saturation level increases with increasing oxygen concentration up to an oxygen concentration of about 0.08 wt-%, becoming constant for oxygen concentrations above this value.

2) The total amount of nitrogen absorbed is the result of two mutually independent processes: inflow of nitrogen through the interface between the arc and the liquid metal, and outflow of ni-

trogen through the entire outer surface of the liquid metal. Oxygen influences the nitrogen absorption predominantly through its effect on the outflow rate. The effect of oxygen on the inflow rate appears to be negligibly small.

3) The role of oxygen can be understood by assuming that oxygen forms a layer on the surface of the liquid metal that hampers the passage of nitrogen atoms. Directly below the arc, this layer is virtually destroyed by the arc plasma, and consequently, the inflow of nitrogen is only slightly affected. Outside the arc, the layer remains intact, which results in a considerable reduction of the outflow rate.

## References

1. Blake, P. D. 1979. *Welding Res. Int.* 9:23–56.
2. Kobayashi, T., Kuwana, T., and Kikuchi, Y. 1967. *Welding in the World* 5:58–72.
3. Uda, M., and Wada, T. 1968. *Trans. Nat. Res. Inst. for Metals* 10:79–91.
4. Verhagen, J. G., Ouden, G. den, Liefkens, A., and Tichelaar, G. W. 1970. *Metal Constr.* 2:135–143.
5. Blake, P. D., and Jordan, M. F. 1971. *J. Iron & Steel Inst.* 209:197–200.
6. O'Brien, J. E., and Jordan, M. F. 1971. *Metal Constr.* 3:299–303.
7. Uda, M., and Ohno, S. 1973. *Trans. Nat. Res. Inst. for Metals* 15:20–28.
8. Ishizaki, K. 1985. IIW Doc. 212-619-85.
9. Kuwana, T., and Kokawa, H. 1986. *Trans. Jap. Weld. Soc.* 17:20–26.
10. Kuwana, T., and Kokawa, H. 1988. *Trans. Jap. Weld. Soc.* 19:92–99.
11. Ouden, G. den, and Griebing, O. 1989. *Proc. 2nd Intern. Conf. on Recent Trends in Welding Science and Technology*. Gatlinburg, Tenn., pp. 431–435.
12. Pehlke, R. D., and Elliott, I. F. 1960. *Trans. AIME* 218:1088–1101.
13. Ouden, G. den. 1977. *Philips Welding Rep.* 13:1–11.
14. Inouye, M., and Choh, T. 1968. *Trans. Iron & Steel Inst. of Japan* 8:134–145.
15. Kozakevitch, P., and Urbain, G. 1963. *Mémoires Scientif.* 60:143–156.
16. Lancaster, J. F. (Ed.). 1986. *The Physics of Welding*. Pergamon Press, Oxford, U.K.

## Basis of Current Dynamic Stress Criteria for Piping

By G. C. Slagis

WRC Bulletin 367  
September 1991

The evolution and development of the ASME Boiler and Pressure Vessel Code requirements for seismic design of piping are documented. The development of analytical methods and regulatory requirements for seismic design are reviewed.

Publication of this report was sponsored by the Pressure Vessel Research Council of the Welding Research Council, Inc. The price of WRC Bulletin 367 is \$40.00 per copy, plus \$5.00 for U.S. and \$10.00 for overseas, postage and handling. Orders should be sent with payment to the Welding Research Council, Room 1301, 345 E. 47th St., New York, NY 10017.